# **Chemical Engineering & Process Techniques**

#### **Research Article**

# A Fluorescent Probe with Activated Dual-Recognition Sites for Detecting Nitrite in a Neutral Medium

# Junxian Zhou, Changshuo Zhang, Lusen Chen, Xiaoling Qin, Lujie Xu, and Fuchun Gong\*

College of Chemistry and Pharmaceutical Engineering, Changsha University of Science and Technology, China

#### \*Corresponding author

Fuchun Gong, College of Chemistry and Pharmaceutical Engineering, Changsha University of Science and Technology, China, Tel: +86-0731-85258733

Submitted: 05 July, 2025
Accepted: 08 October, 2025
Published: 09 October, 2025

**ISSN:** 2333-6633 **Copyright** 

© 2025 Zhou J, et al.

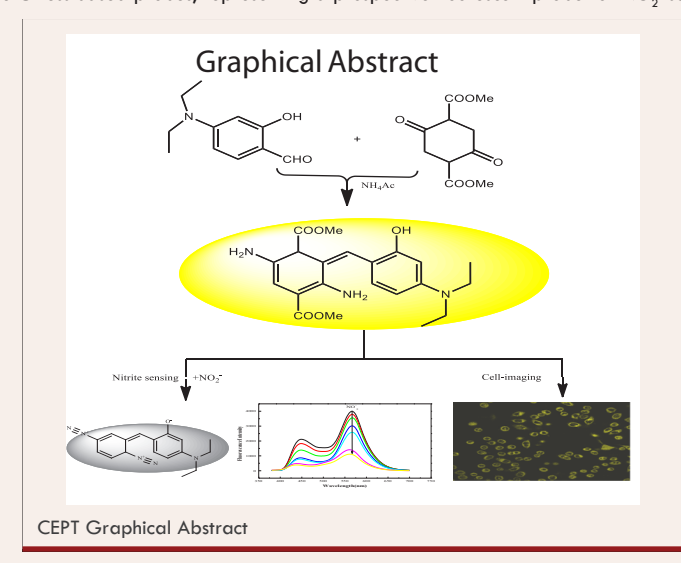
OPEN ACCESS

#### **Keywords**

Diaminosubstituted Cyclohexadiene; Synthesis;
 Decarboxylation; Nitrite Sensing; Cell-Imaging

#### Abstract

Nitrite (NO<sub>2</sub>) has been widely used in the food and beverages manufacturing processes. It has been identified as a significant threat chemical to human health and heavily assayed in the field of food safety and water quality control. Using Griess reaction to produce dizaonium salt or initiate further cyclization reaction for signalling are the mainstream strategies for NO<sub>2</sub> sensing. However, conventional amino recognition reaction sites often suffer from extensive incubation time and strong acidic medium. Herein, we developed a diaminosubstituted cyclohexadiene fluorescent probe (DAE) by "multicomponent one pot" synthesis. The as prepared probe DAE is endowed with two amines activated by carboxylic acid ester, making it easy to react with NO<sub>2</sub>. DAE exhibited sensitive and specific response to NO<sub>2</sub> in a weak acid medium (acetonitrile PBS system, pH 6.0) due to the activation of adjacent carboxylic ester groups. A DAE based method for the detection of NO<sub>2</sub> was established, offering a LOD of 7.75 nM. Preliminary mechanism investigation reveals that this specific recognition reaction resulted from the NO<sub>2</sub> mediated diazotization and decarboxylation ester of DAE. Moreover, the DAE loaded paper device was fabricated and employed to monitor NO<sub>2</sub>, featuring simplicity and high efficiency. DAE was also successfully employed for fluorescence imaging in live cells, displaying good biocompatibility and excellent imaging ability. Overall, the developed probe DAE has addressed the difficulties of long incubation time and strong acid condition associated with the Griess based probes, representing a prospective fluorescent probe for NO<sub>2</sub> sensing.



# Highlights

- 1. A diaminosubstituted cyclohexadiene fluorescent probe (DAE) was developed.
- 2. DAE contains activated dual recognition sites for the reaction with NO.
- 3. DAE shows highly sensitivity and selectivity toward NO<sub>2</sub> in a weak acid medium.
- 4. DAE was also employed for fluorescence imaging in live cells.

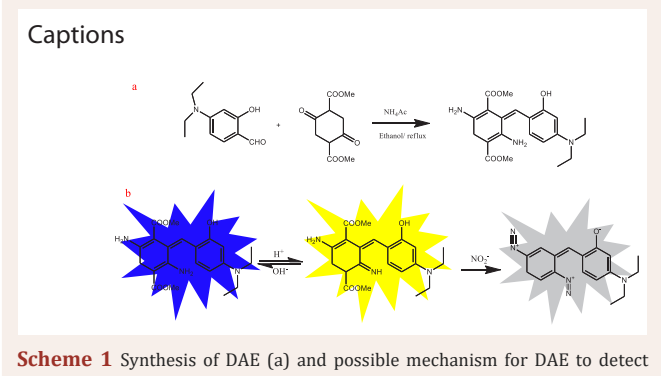
# **INTRODUCTION**

Nitrite (NO<sub>2</sub>), is generally used as a food additive to improve the color and flavor of the preserved meat, bean curd and szechuan pickle [1,2]. It can also act as a preservative to inhibit the growth of some bacteria, extending the shelf-life of meat products [3,4]. Meanwhile, the ageing of cooked leftovers and the fermentation process in curing preparations may elicit the generation of NO<sub>2</sub> [5,6]. Extensive studies indicated that the long term accumulation of NO<sub>2</sub> could endanger human health. The excessive intake of NO<sub>2</sub> existing in food and drinking water can result in various diseases, such as spontaneous abortions, infant methemoglobinemia, intrauterine growth restriction and central nervous system defect of fetuses [7-10]. In addition, NO<sub>2</sub> is also a carcinogenic species because that the NO<sub>2</sub> can react with the ingredients in food (amines and its derivatives) to produce highly carcinogenic N-nitrosamine in the gastric acid environment [11,12]. The nitrosamines can also get into the fetus through the placenta and cause lethal hazard to the fetus, such as growth retardation, teratogenic, premature delivery, defects, etc [13,14]. Therefore, the development of the NO<sub>2</sub> assays is of significantly importance in food processing industries, medical science and environmental field.

Up to now, various instrument based methods are available for NO<sub>2</sub> detection, such as chromatography [15], electrochemical [16], capillary electrophoresis [17] and spectrophotometry [18]. However, many of the mentioned methods are not propitious for routine analysis of NO<sub>2</sub>in food or environmental samples because of that some of them suffer from tedious sample preparation, evident background interference, as well as time consuming and high cost. In the last few years, fluorescent probe-based methods have drawn tremendous attention owing to their high specificity, simple operation, fast response, low cost and non destructive analysis [19,20]. Up to now, plentiful fluorescent probes for NO<sub>2</sub> have been reported [21-24]. Most of the NO<sub>2</sub> specific probes is mainly based on the diazotization of amino group [25,26], which contains two main types of reactions, Griess reaction of monoamino group and the cyclization reaction of o phenylenediamine to produce benzotriazole [27-30]. Due to the low stability of azide species, these detection systems usually suffer from the restrictions, such as interference from cellular contents, binding of metal ions, involving in multiple reagents, and moderate LOD in related processes such as NO determinations [31-33]. Therefore, to develop new fluorescent dyes that monitor NO2 through alternative recognition pathways is important for designing new NO<sub>2</sub> -probes.

The mainstream strategy for the design of NO<sub>2</sub> -specific probes is to graft an amino group on a dye molecule or link an ophenylenediamine with a fluorophore for the oxidation reaction with NO<sub>2</sub> [33-38]. These approaches usually involve in tedious synthesis steps such as the construction of the phosphors and the coupling of dyes with amino moieties. In recent years, fluorescent nanostructures such as Heavy Metal Nanoclusters (HMN) [39], Semiconductor Quantum Dots (SQD) [40], Carbon Dots (CD) [41], and Metal Organic Framework Materials (MOF) [42], have been introduced in the design of nitrite probes. However, these nanofluorophore based probes display some drawbacks in practical routine applications. For examples, the gold nanocluster [43], and polyethylenimine capped CdS quantum dotbased [44], probes for the detection of NO<sub>2</sub> are severely disturbed by some anions. The stability and biotoxicity of HMNs and SQDs have not been effectively solved [45]. Besides, these nano probes require complicated preparation.

To overcome the above mentioned drawbacks, here we presented a diaminosubstituted cyclohexadienebased probe (DAE) for detecting NO<sub>2</sub>. The probe DAE was strategically synthesized by the sample "one-pot" reaction of dimethyl 2,5<sup>-</sup>dioxocyclohexane-1,4-dicarboxylate ammonium acetate and 4-(diethylamino)-2hydroxybenzaldehyde (Scheme 1). DAE exhibits strong orange yellow fluorescence in a weak acid system (acetonitrile PBS, pH 6.0). After reacting with NO<sub>2</sub>, DAE produced a product of azolation, eliciting the decrease in emission. From this basis, a highly selective and sensitive method for NO<sub>2</sub> detection was established. A DAE loaded paper device was also fabricated and employed for monitoring NO<sub>2</sub> ions in actual food samples. Furthermore, DAE was successfully applied to fluorescence imaging in live cells. The developed probe provides a more practical method for the detection of NO<sub>2</sub> and fluorescence imaging in live cells, indicating good application prospects.





# **EXPERIMENTAL METHOD**

#### Materials and instruments

All chemicals and reagents were obtained from commercial suppliers and used without further purification in this study. Dimethyl 2,5-dioxocyclohexane-1,4-dicarboxylate was purchased from Bide Pharmatech Ltd. (Shanghai, China). 4-(diethylamino)-2-hydroxybenzaldehyde and ammonium acetate were purchased from Macklin (Shanghai, China). Sodium nitrite was obtained from Sigma-Aldrich Chemical Company (Shanghai, China). All ionic solutions were prepared from their sodium and chloride salts, respectively. Deionized water was used in all experiments.

The 1H NMR and 13C NMR spectra were measured on an AV-600 spectrometer (Bruker, Switzerland) with tetramethylsilane (TMS;  $\delta$  = 0ppm) as an internal reference. The ESI mass spectrum was recorded with the LTQ Orbitrap XL mass spectrometer. The UV-visible absorption spectra were measured on a UV-1800 spectrophotometer (Shimadzu, Japan). Fluorescence spectra were recorded on an F-7000 spectrophotometer (Hitachi, Japan). The fluorescence quantum yields were detected by HORIBA FluoroMax-4P (HORIBA Jobin Yvon). Fluorescence images of cells were taken using a confocal laser scanning microscope (Nikon, Tokyo, Japan).

# Synthesis of probe DAE

2,5<sup>-</sup>diamino-3-(4<sup>-</sup>(diethylamino)-2-hydroxybenzylidene) cyclohexa-1,5-diene-1,4-dicarboxylate(DAE)wassynthesized according to literature with minor modification [46]. In short, dimethyl 2,5-dioxocyclohexane-1,4-dicarboxylate (2.3 g, 10 mM), 4-(diethylamino)-2-hydroxybenzaldehyde (1.9 g, 10 mM) and ammonium acetate (5.4 g, 70 mM) were dissolved in 30 mL ethanol. The mixture is refluxed under stirring for 4 h. After cooling to room temperature, the resulting mixture was filtered and washed with cold ethanol, obtaining crude products. Finally, the product was further recrystallized from ethanol and dried at 60 °C to afford light yellow powder (4.3 g, 76.6%). 1H NMR (400 MHz, DMSO) δ 11.91, 7.83, 6.34, 6.32, 6.04, 6.03, 3.73, 3.58, 3.42, 3.40, 3.10, 3.08, 3.07, 3.05, 3.04, 3.03, 1.11, 1.09. 13C NMR (101 MHz, DMSO) δ 171.38, 167.31, 155.43, 147.95, 144.05, 120.79, 118.01, 114.78, 104.89, 96.35, 52.94, 52.19, 44.58, 12.86. FTMS: m/z calculated for C<sub>2</sub>1H<sub>2</sub>4N<sub>2</sub>O<sub>6</sub> ([M+]):401.16; found 401.17

In addition, the structure of DAE was also characterized using XPS analysis. As shown in Figure S4, the probe DAE exhibits three distinct signals at 282.26, 396.24 and 529.81 eV in the survey spectrum, which corresponds to C1s, N1s and O1s peaks, respectively. Since the carbon atoms present

in DAE are faced to three chemical microenvironments, three different bands at 284.80, 286.30, 289.00 eV can also be observed in the high resolution C1s spectrum, attributing to the C·O, C·N, and C·O·C=O species respectively. There are three bands at 533.30, 531.80 and 530.30 eV appear in high resolution spectrum of O1s, which belongs to C-O-C=O, C=O, C-O and binding atoms, respectively. The N1s spectrum showed two obvious peaks at 401.40, and 399.20 eV, related to C-NH<sub>2</sub>, and C-N bonds, respectively.

#### **General spectra measurements**

For the preparation of stock solution of DAE (10<sup>-3</sup> M), 0.04 g DAE was dissolved in 100 mL acetonitrile-PBS mixed system (acetonitrile: PBS = 6:4, v/v, pH 6.0). The probe solution was stored at 4 °C in a refrigerator. When used for detecting NO<sub>2</sub> or the other competitive ions, 10 mL of DAE solution was added with 10 L PBS (10 mM) to form an acetonitrile<sup>-</sup>DAE<sup>-</sup>PBS system. After uniform mixing, various concentrations of NO2 solutions were spiked and added into the acetonitrile -DAE-PBS system. For the preparation of  $NO_2$  stock solution, 0.07 g sodium nitrite was added into a 100 mL volumetric flask with deionized water to give the stock solution of NO<sub>2</sub> with a concentration of 1×10<sup>-3</sup> M. The other solutions containing competitive species (1×10<sup>-2</sup> M) were prepared by dissolving their responsive compounds with deionized water. The absorbance and fluorescence spectra were obtained as an average of three times independent measurements. The intensity of the fluorescence values was determined to build a linear calibration curve. The response of the acetonitrile PBS DAE system to the other ions was also captured to verify the specificity for NO<sub>2</sub> detection.

# Preparation of DAE-loaded test paper

The DAE loaded test paper was prepared by immersing the circular filter paper (3.0 mm diameter) into an acetonitrile solution containing DAE (150  $\mu M)$  for 30 min and then dried gently. Before the usage, the DAE immobilized paper was added with 1.0  $\mu L$  PBS buffer (pH 6.0) to obtain the PBS DAE loaded test paper device. During sample testing, the paper was soaked into the aqueous solution containing nitrite ions for 15 s and dried in air. Under a 365 nm handheld UV lamp, blue or white fluorescence appears in the DAE loaded test papers and the images were then taken.

# Detection of NO2- in real samples

All food samples were obtained from local supermarket in Changsha. Meat product ( $10.0\,\mathrm{g}$ ) was weighed in a beaker, followed by the addition of a 15 mL borax solution (5%) and 250 mL hot water. The mixture was heated in a boiled

water bath for 20 min. 10 mL  $\rm K_4[Fe(CN)_6]$  solution and 10 mL Zn  $\rm (CH_3COO)_2$  solution were then added to precipitate the proteins. The resulting mixture was diluted to 500 mL with ultrapure water, followed by filtration through filter paper (28 cm). The filtrate (1.0 mL) was measured using the method described in Section 2.3.

The cleaned and dried pickled vegetables were weighed in a beaker (10 g), a 15 mL borax solution (5%) and 250 mL of ultrapure water were then added. The mixture was incubated in a boiled water bath for 25 min. After cooling to room temperature, 235 mL ultrapure water was added. After filtration, the filtrate (1 mL) was place into a 10 mL cuvette and measurement with the method described in Section 2.3.

# Fluorescence imaging

The application of DAE to cell-imaging was investigated using laser scanning confocal microscopy (CLSM). (1) Cell expansion: The primary HeLa cells were pulled into a 18 mm glass bottom dishes at a density of 5.0×10<sup>4</sup> cells/ dish, enabling them to grow naturally in DMEM medium (10% acetonitrile PBS mixed system buffer, 1% penicillin streptomycin and 5% CO<sub>2</sub>), under humidified atmosphere at 37 °C for overnight. (2) Cell staining: The original culture medium was removed and added a fresh medium solution (2.5 mL) containing 25  $\mu M$  DAE and the HeLa cells were further incubated for 12 h. The colored cells were then isolated from the medium and washed with an acetonitrile-PBS mixed system buffer (20 mM, pH 3.5). (3) Cytological observation: After washing with the same icecold acetonitrile-PBS mixed system buffer for three times, the stained cells were observed using CLSM, cognizing the intracellular distribution of DAE against HeLa cells.

#### Theoretical calculation

The geometric configurations in the ground states of DAE and its product were fully optimized by the density functional theory (DFT) and the time dependent density functional theory (TDDFT), respectively. The B3LYP method and 6·311++G (d, p) higher order basis set were employed for the calculations. HOMO and LUMO were calculated by the optimized structure. All calculations in this work were acquired from Gaussian 03 W program package on a personal computer and some of the data are obtained using ORCA 4.0.1.

#### **RESULTS AND DISCUSSION**

# Design and synthesis of probe DAE

Numerous fluorescent probes for detecting NO<sub>2</sub> have been developed based on Griess reaction [47-49].

Unfortunately, the conventional diazotization based probes for NO2 involve in external agents and require a strong acidic medium. It has been reported that nitrogen dioxide can react with olefinic bonds to form oxime groups and remove carboxylic acid ester [50]. Inspired by this finding, we developed a novel colorimetric and fluorometric probe DAE. In this probe, there are two amino groups for the reaction with  $NO_2^-$  and the ortho ester groups for the activation of the amino groups. The probe DAE was synthesized by the "multi-component one pot" reaction of dimethyl 2,5-dioxocyclohexane<sup>-</sup>1,4<sup>-</sup>dicarboxylate 4-(diethylamino)-2-hydroxybenzaldehyde with ammonium acetate (Scheme 1a). The probe DAE was fully characterized by 1H NMR, 13C NMR, ESI Mass and XPS (Figure S1-S4).

#### Characteristic spectra and response of DAE

To further insight into the spectral properties and response behavior of the prepared probe DAE, the absorption and fluorescence measurements were carried out. Firstly, we investigated UV-visible absorption of DAE and DAE+NO<sub>2</sub>. As shown in Figure 1a, there are two obvious absorption peaks located at 355 and 415 nm, respectively. When a 10  $\mu M$   $NO_2^-$  solution was added, the absorption peak of the acetonitrile PBS DAE system (pH 6.0) at 355 nm was tremendously decreased and a new absorption band at 450 nm appeared. At the same time, the concomitant color of the resulting solution changed from yellow to blue. Next, we measured the fluorescence spectra of DAE and its response to NO<sub>2</sub>. The fluorescence of DAE showed two strong peaks at located 450 and 565 nm when excited with 355 nm. As expected, the fluorescence at 450 and 565 nm was significantly quenched in the presence of 35 μM NO<sub>2</sub> (Figure 1b). The effect of pH on the fluorescence of DAE was also investigated. As shown in Figure 1c, the fluorescence of DAE is strong at a lower pH. Figure 1d outlines the effect of solvents on the fluorescence spectra of DAE. It displays that alcohol solvents can weaken fluorescence at 565 nm and enhance the fluorescence at 450 nm. In addition, we further investigated the effect of reaction time on the fluorescence quenching of DAE. The results showed that the fluorescence quenching of acetonitrile PBS-DAE system (pH 6.0) with the addition of NO<sub>2</sub> reaches its maximum value in 2 min and the extensive reaction time cause the plateau (Figure S5).

Next, the concentration titration experiments were carried out. As shown in Figure 2a, the absorption peak at 355 nm gradually decreased and a new absorption peak at 450 nm appeared with the addition of increasing amount of NO<sub>2</sub>. The absorption intensity of the probe DAE at 355 nm showed a good linear relationship with

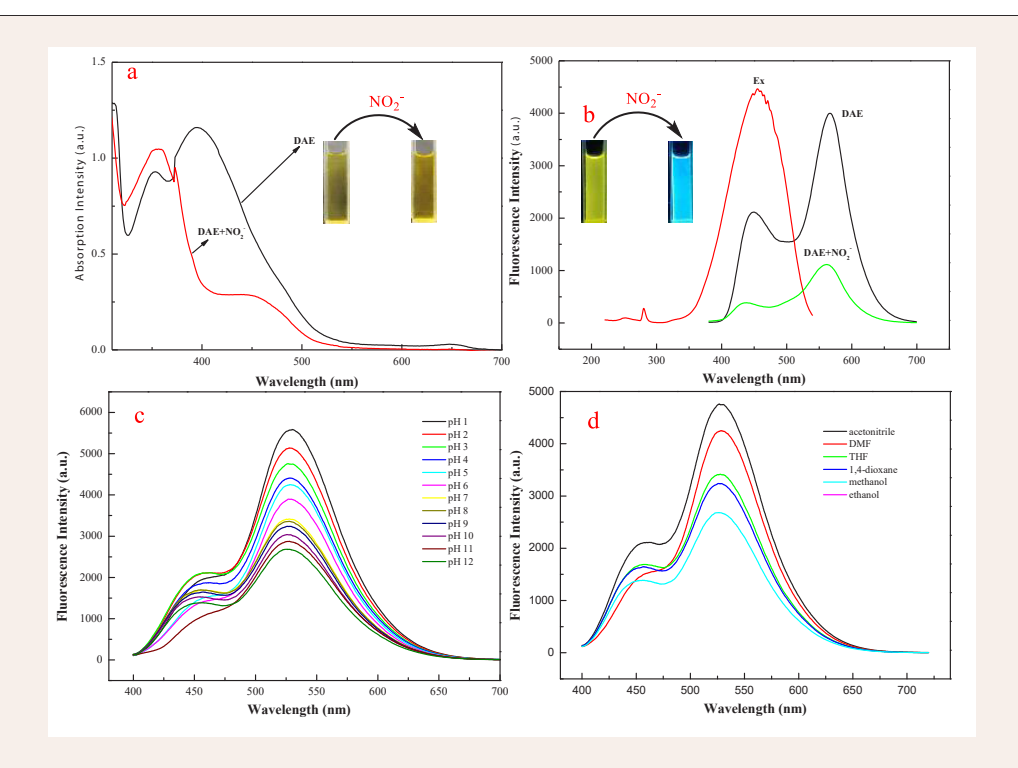
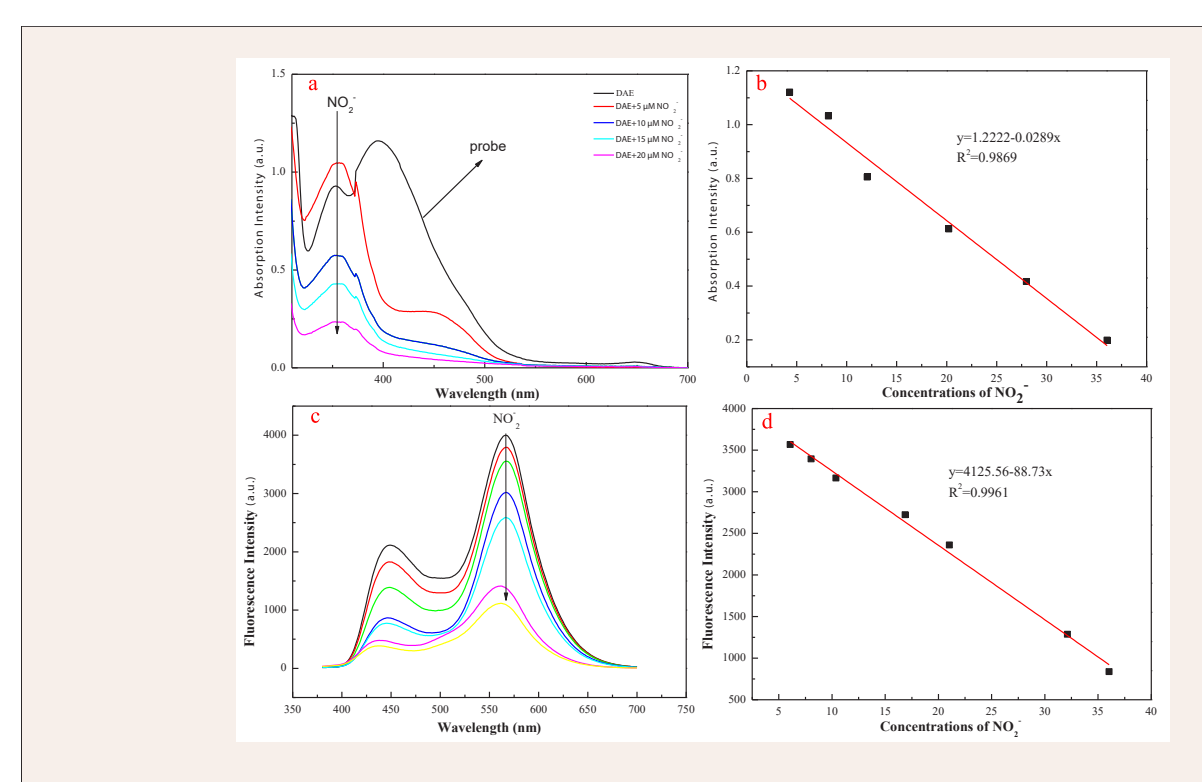


Figure 1 Absorption and fluorescence spectra of DAE and the DAE in the presence of  $NO_2$ . (a): The absorption spectra of DAE and the DAE with the addition of  $NO_2$  in acetonitrile-PBS mixed system (6/4, v/v, pH=6.0). (b): Excitation and emission spectra of DAE in the same acetonitrile-PBS system. (c): The fluorescence spectra of DAE in different pH solutions (d): Fluorescence spectra of 10  $\mu$ M DAE in different solvents.



**Figure 2** Absorption spectra (a) and Fluorescence spectra (c) of the probe DAE toward the various concentrations of  $NO_2$  (final concentration: 0, 5, 7.5, 10, 12.5, 20, 32.5, 37.5  $\mu$ M). The linear plots of the absorbance (b) (Abs 355 nm) and fluorescence (d) (Ex 450/Em 565 nm) againsts the concentrations of  $NO_2$  within 0-40  $\mu$ M.

the concentration of NO $_2$  ranging from 0 to 40  $\mu$ M (R² = 0.9869), and the detection limit was calculated as 47.15 nM (Figure 2d). In addition, the absorbance intensity showed no further decrease once 2 equivalents of NO $_2$  was present in solution, suggestive of a 1:2 dose response relationship for DAE to NO $_2$  (Figure S6). The fluorescence response of probe DAE to NO $_2$  ions was also evaluated by concentration titration experiments. The fluorescence intensities fit linear relationship with the NO $_2$  concentrations of 10·40  $\mu$ M was acquired (Figure 2c). Subsequently, the detection limit (LOD) for NO $_2$  was calculated as 7.75 nM (3 $\sigma$ /k), which is lower than that of the reported UV visible method [51]. This indicated that the excellent sensitivity of probe DAE will provide a new sensing strategy for NO $_2$  detection.

# **Selectivity**

To investigate the selectivity and anti-interfering performance of this probe, we examined the fluorescence response by adding NO $_2$ - and competitive anions to the acetonitrile PBS DAE system (pH 6.0) under the same conditions. As shown in Figure 3a and Figure S7, S8, the interfering species, including F-, Cl-, Br-, I-, HSO $_4$ -, SO $_4$ -HPO $_4$ -, NO $_3$ -, HCO $_3$ -, CO $_3$ -, S $_2$ O $_3$ -, S $_2$ O $_5$ -, SCN-, S $_2$ -, N3- can lead to negligible change of the PBS DAE system. The concentrations of these interfering components are 20  $\mu$ M.

Only  $\mathrm{NO_2}^-$  can cause significant fluorescence quenching. In addition, in coexistence with  $\mathrm{NO_2}^-$ , these competitive anions do not elicit the change in fluorescence spectra (Figure 3b). Moreover, the fluorescence of the PBS-DAE systems were visibly altered by  $\mathrm{NO_2}^-$  exposed to ultraviolet radiation at 365 (as shown in Figure 3c). In contrast, the other anions did not resulted in change in fluorescence of the sensing system. These, results indicated that this DAE-based method had high selectivity for  $\mathrm{NO_2}^-$  detection. Conclusively, the highly specific  $\mathrm{NO_2}^-$  detection was achieved based on the double reactions of DAE with  $\mathrm{NO_2}^-$ , which endows the proposed fluorescent probe with satisfactory anti-interference over other competitive anions.

### Analytical application in real food samples

As a ubiquitous harmful substance in foods, the analysis of  $\mathrm{NO_2}^-$  in actual samples is particularly significant. So, we determined the  $\mathrm{NO_2}^-$  residue in six food samples using the probe DAE. The sample preparations are described in the Experimental section. The determination of  $\mathrm{NO_2}^-$  contents in the food samples by spiked recovery, and the results were presented in Table 1. As shown in this table, the satisfactory recoveries (99.25% to 104.31%) can be achieved, and all RSD values are less than 0.41%. What's

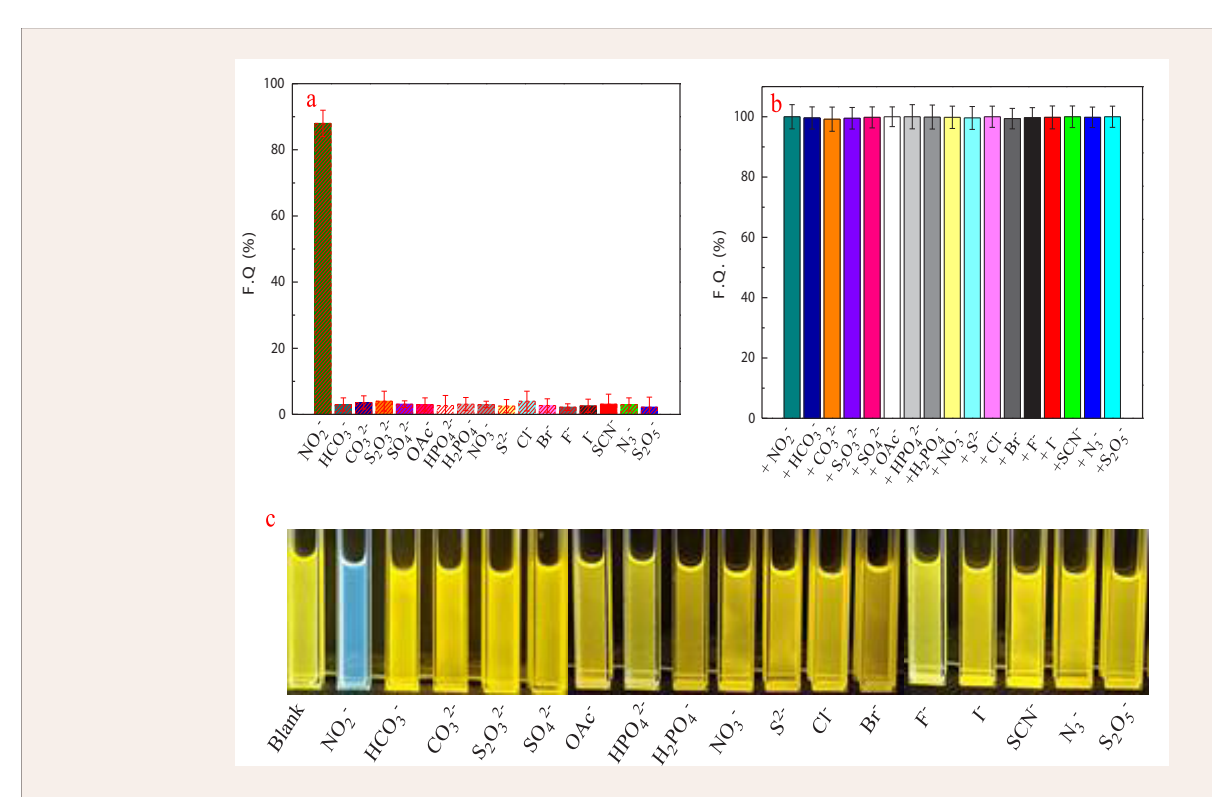


Figure 3 The selectivity (a) and anti-interference (b) of the probe DAE (10 μM). Fluorescence images (c) of the probe DAE (10 μM) upon adding  $25 \mu M NO_2$  and different competing ions. The solution is an acetonitrile-PBS system (acetonitrile-PBS = 6:4, v/v, pH = 6.0).

Table 1: Determination results of the NO, content in real food samples using probe DAE and UV-visible spectrophotometric method

| Samples           | NO2 added (µM.L-1) | NO <sub>2</sub> · found (μM.L·1) | Recoveries | RSD  | UV-visible method | P*    |
|-------------------|--------------------|----------------------------------|------------|------|-------------------|-------|
| •                 | 2 5 7              | 2 0, ,                           | (%)        | (%)  |                   |       |
|                   | 0                  | 1.92                             | -          | -    | 1.91              |       |
|                   | 5                  | 6.97                             | 100.72     | 0.26 | 6.95              |       |
|                   | 10                 | 11.87                            | 99.58      | 0.42 | 11.88             |       |
| Sausage           | 20                 | 22.06                            | 100.64     | 0.33 | 21.98             |       |
|                   | 40                 | 42.15                            | 100.55     | 0.28 | 42.07             |       |
|                   | 0                  | 3.02                             | -          | -    | 3.05              |       |
|                   | 5                  | 7.96                             | 99.25      | 0.28 | 7.98              |       |
|                   | 10                 | 13.12                            | 100.77     | 0.37 | 13.10             |       |
| Spiced beef       | 20                 | 23.01                            | 99.91      | 0.33 | 23.03             |       |
|                   | 40                 | 43.07                            | 100.10     | 0.41 | 43.05             |       |
|                   | 0                  | 3.51                             | -          | -    | 3.53              |       |
|                   | 5                  | 8.23                             | 96.71      | 0.33 | 8.27              |       |
| Luncheon          | 10                 | 13.44                            | 99.48      | 0.29 | 13.40             |       |
|                   | 20                 | 23.86                            | 101.49     | 0.35 | 23.72             | >0.05 |
|                   | 40                 | 44.02                            | 101.17     | 0.26 | 43.98             |       |
|                   | 0                  | 1.19                             | -          | -    | 1.21              |       |
| Preserved mustard | 5                  | 6.23                             | 100.65     | 0.34 | 6.27              |       |
|                   | 10                 | 11.31                            | 101.07     | 0.27 | 11.31             |       |
|                   | 20                 | 21.07                            | 99.43      | 0.36 | 21.13             |       |
|                   | 40                 | 41.16                            | 99.93      | 0.31 | 41.25             |       |
| Pickled cabbage   | 0                  | 1.81                             | -          | -    | 1.79              |       |
|                   | 5                  | 6.77                             | 99.41      | 0.37 | 6.81              |       |
|                   | 10                 | 11.92                            | 100.93     | 0.41 | 11.80             |       |
|                   | 20                 | 21.97                            | 100.73     | 0.33 | 21.90             |       |
|                   | 40                 | 42.01                            | 100.48     | 0.29 | 21.93             |       |
|                   | 0                  | 1.60                             | -          | -    | 1.62              |       |
| Dried radish      | 5                  | 6.67                             | 101.11     | 0.23 | 6.63              |       |
|                   | 10                 | 11.65                            | 104.31     | 0.37 | 11.59             |       |
|                   | 20                 | 21.48                            | 99.44      | 0.41 | 21.65             |       |
|                   | 40                 | 41.72                            | 100.29     | 0.27 | 41.61             |       |

 $P^*$ : significant difference. The sig value is usually expressed as P > 0.05, and the difference is not significant; 0.01 < P < 0.05 indicates significant difference; P < 0.01 indicates that the difference is extremely significant.

more, these results from the present DAE based method agree with those obtained using Griess reaction based colorimetry, and the relative error between our proposed probe based approach and the standard method is lower than 5 %. From the data in Table 1, we can also see that this method is suitable for the quantification of  $NO_2$  in a variety of foods and the probe DAE provided a good method to detect  $NO_2$  in the food samples.

# Monitoring of $NO_2$ - using DAE-loaded paper device

To make the probe based method more convenient, a DAE loaded paper device was fabricated as descripted in Section 2.4. As shown in Figure 4a, the obvious fluorescent color gradient from yellow to blue and then to white could be observed by the naked eye upon the addition of different concentrations of  $\mathrm{NO_2}^{\circ}$ . The results indicated that the DAE loaded device could be employed for tracking  $\mathrm{NO_2}^{\circ}$ .

Based on the above approach, time dependent detection of  $\mathrm{NO_2}^-$  content in different meat and vegetable samples, as well as with different storage time were monitored by the proposed DAE-loaded paper device. As shown in Figure 4b, the  $\mathrm{NO_2}^-$  contents of the canned meat and pickled vegetables stored at 25±1 °C for 4 days display slight change which were lower than the maximum residue level (20 mg.kg<sup>-1</sup>)

[52]. The results indicated that the  $NO_2$  contents in the canned food and pickled vegetables continues to increase during their storage. This facile device can used to monitor the changes in  $NO_2$  contents of foodstuff during storage.

# Sensing mechanism

To further unveil the recognition mechanism for DAE to sense  $\mathrm{NO_2}$ , the 1H NMR spectra of DAE and the products of DAE+ $\mathrm{NO_2}$  were investigated. As shown in Figure 5a, DAE exhibits the characteristic H signals at 7.27, 7.42 ppm ( $\mathrm{^{1}NH_{2^{\prime}}}$ , -OH) and their hydrogen bond forms at 11.89 ppm. Upon addition of  $\mathrm{NO_2}$ , the H signals for  $\mathrm{^{1}NH_2}$  and -OH of DAE were found to disappear (Figure 5b). To further verify this result, we conducted infrared testing. As shown in Figure 5c, the DAE structure showed strong  $\mathrm{^{1}NH_2}$  (3431.30 cm $^{-1}$ ) and -OH (3322.08 cm $^{-1}$ ) characteristic peaks. After reaction with  $\mathrm{NO_2}$ , the original characteristic peak of DAE disappeared, which agree with the results of NMR measurements. These results suggest the occurrence of azidation of the amino and the disappearance of carboxylic ester groups in the DAE molecules.

The product of DAE+  $NO_2^-$  was also certified by electrospray ionization mass spectrometry. In the presence of  $NO_2^-$ , a predominant peak at m/z 308.07 was

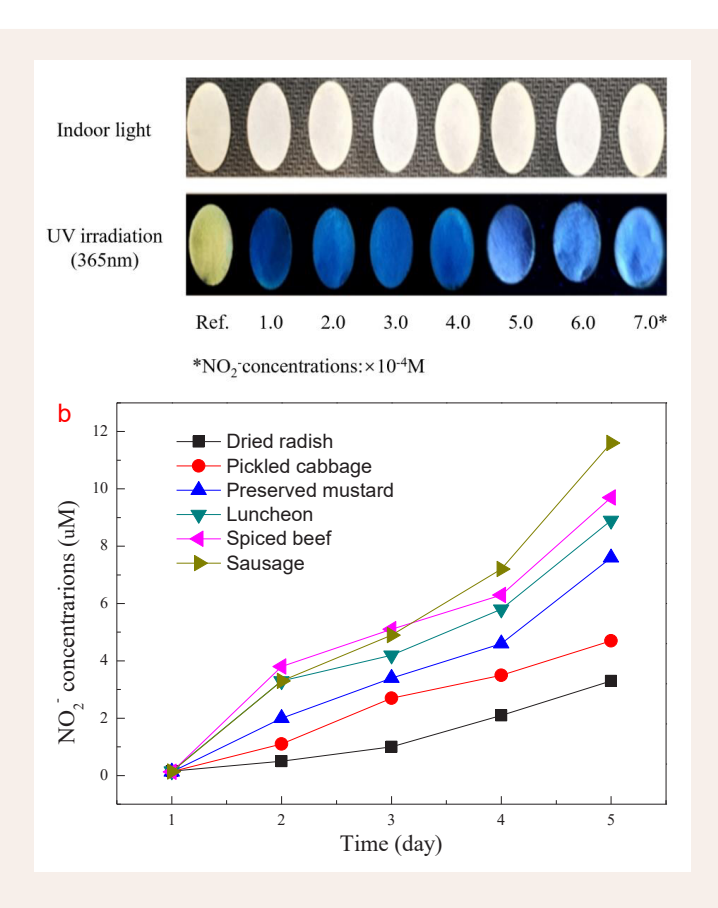


Figure 4 Fluorescence images of the DAE-loaded paper device upon adding different concentrations of NO2- (a). The DAE-loaded paper device was used to evaluate the effect of ambient temperature  $(25 \pm 1 \text{ oC})$  storage on the NO2- concentrations of different food samples (b).

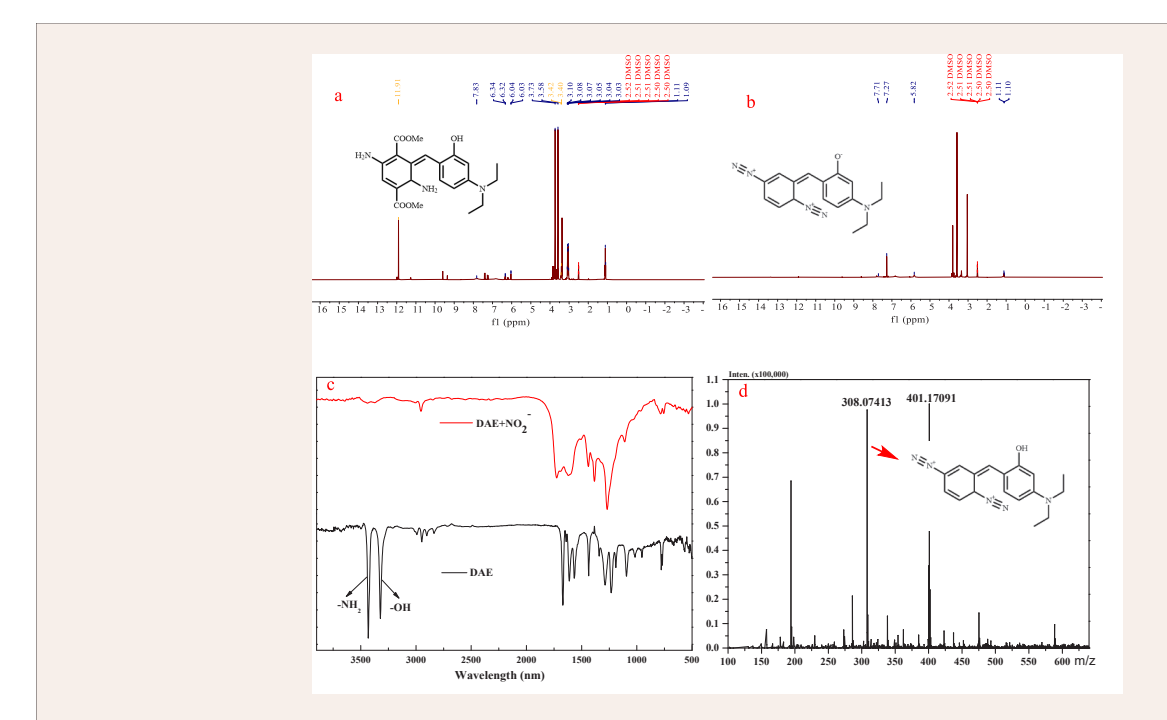


Figure 5 1H NMR (400 MHz) spectrum of the probe DAE (a) and the products of DAE-NO2-(b) in DMSO-D6; The infrared spectroscopies of DAE and the products of DAE-NO2-(c); The mass spectra of the isolated products (d).

observed in the MS spectrum of the products ( $C_{17}H_{18}N_5O$ , [M $^+$ ]), calculated data: 308.15) (Figure 5d), which can be attributed to the bis diazo product resulted from the reaction of DAE with  $NO_2$ . Thus, it was demonstrated that the generation of the bis diazo products, which is responsible for the optical signal changes induced by  $NO_2$ . In addition, we measured the fluorescence response of the probe DAE reacting with different equivalents of  $NO_2$ . The result indicated that the fluorescence quenching of DAE reaches the plateau when the amount of  $NO_2$  added is greater than twice the equivalent of the probe. The binding stoichiometry of DAE and  $NO_2$  was identified as 1:2 (Figure S6).

#### Theoretical calculations

To further understand the optical behavior and the response mechanism of DAE towards NO<sub>2</sub>, the density functional theory (DFT) based calculations were carried out. For calculating the Frontier orbitals of DAE and its product, the B3LYP functional and the 6-311G (d) basis set were employed in this study. As shown in Figure 6, the HOMO and LUMO of DAE are located on almost the whole molecule, indicating the charge transfer between the 3 (diethylamino)phenol and diaminosubstituted cyclohexadiene moiety. In the product of DAE+NO<sub>2</sub>, the HOMO is concentrated on diazotized cyclohexadiene moiety; and the LUMO of DAE+NO<sub>2</sub> is located on almost the whole molecule. Therefore, electron withdrawing

cyclohexadiene group could totally quench the fluorescence of the 3-(diethylamino)phenol moiety through PET process. In addition, the energy gap between HOMO and LUMO of DAE+NO<sub>2</sub><sup>-</sup> was calculated to be 2.79 eV, which are is slightly larger than that of DAE (2.23 eV), suggesting no significant difference in absorption peaks among the two compounds.

#### Cell<sup>-</sup>image

As shown in Figure S10, the probe DAE did not cause significant cytotoxicity at the concentrations less than 35  $\mu M.$  Thus, to validate the effectiveness of the probe DAE in binding to proteins, confocal fluorescence microscopic experiments in living cells was carried out. HeLa cells were selected as cell model and stained with DAE for 30 min, followed by treatment with 50  $\mu M$  of  $NO_2$  for 10 min. As shown in Figure 7a, the cells incubated only with DAE showed strong yellow fluorescence. When the stained HeLa cells with DAE were further treated with NO<sub>2</sub>, it exhibited relatively weak fluorescence (Figure 7d). This result indicates that the probe DAE can be ingested into cells and interact with intracellular NO<sub>2</sub>. Moreover, it can also be clearly seen that the ingested dyes are mainly concentrated on the cytoplasmic regions with rich proteins. These results demonstrated that the probe DAE not only can be used to track NO2, but also afford fluorescence image in live cells due to its high affinity to anchor proteins.

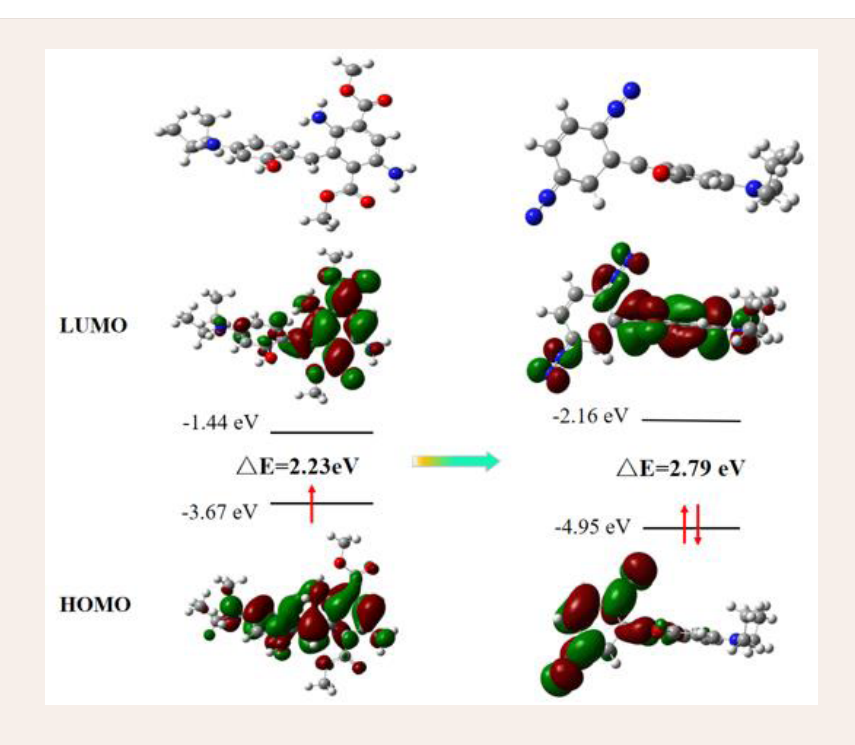


Figure 6 Molecular orbital plots of DAE and the proposed product of DAE+NO,

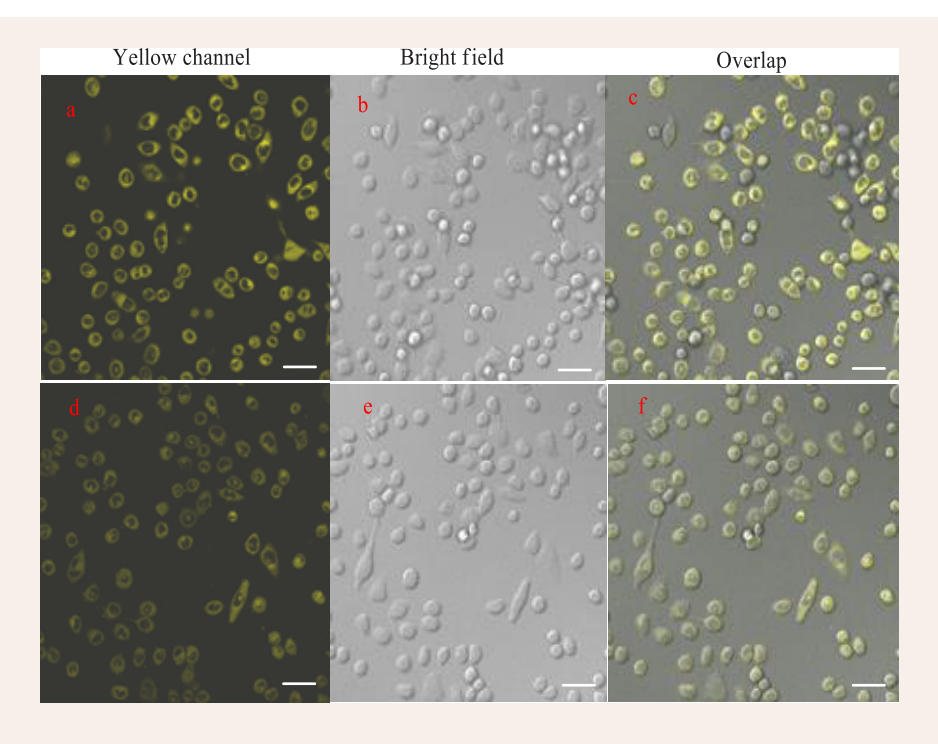


Figure 7 Confocal fluorescence images of HeLa cells. Fluorescence images of HeLa cells stained by probe DAE (5  $\mu$ M, 30 min) only (a, d, c); Fluorescence images of HeLa cells incubated with the probe DAE (5  $\mu$ M, 30 min) and subsequently with NO<sub>2</sub> (50  $\mu$ M, 10 min) (d, e, f).

#### **CONCLUSIONS**

In summary, a NO<sub>2</sub> -specific probe DAE based on a new sensing mechanism was successfully designed and synthesized in this study. In a slight acid medium, DAE can exhibit sensitive response to NO2 in the presence of other competitive species. The spectrofluorometric results indicated that the yellow fluorescence of DAE was gradually decreased with the increase of NO<sub>2</sub> concentrations from 0 to 40 μM, enabling DAE to detect NO<sub>2</sub> quantitatively. The structural identification data demonstrated that the extraordinary response of DAE resulted from the NO<sub>2</sub>mediated diazotization and de esterification reactions. The proposed DAE-loaded paper device can be used for rapid monitoring of NO<sub>2</sub>. In addition, the selective binding of DAE to proteins in HeLa cells was confirmed by confocal microscopy imaging. The present strategy could be useful for designing fluorescent probes for the highly selective and sensitive determination of NO<sub>2</sub> and cell imaging based on the dual site reaction of DAE with NO<sub>2</sub>. The proposed versatile probe DAE can provide a simple and convenient platform for sensing NO<sub>2</sub>.

# **DECLARATION OF COMPETING INTEREST**

The authors declare that they have no known competing financial interests or personal relationships that could have appeared to influence the work reported in this paper.

#### **ACKNOWLEDGEMENTS**

We are very grateful for the support of the Research Foundation of Education Bureau of Hunan Province (No.18A141) and the State Key Laboratory of Bio-organic and Natural Product Chemistry (No. SKLBNPC19250).

# **CREDIT AUTHOR STATEMENT**

Junxian Zhou: Methodology, Formal analysis, Investigation, Writing Original Draft. Changshuo Zhang: Validation, Software, Visualization. Lushen Chen: Conceptualization, Investigation, Visualization. Xiaoling Qin: Investigation, Visualization. Lujie Xu: Writing Review & Editing, Investigation. Fuchun Gong: Conceptualization, Resources, Supervision, Funding acquisition, Writing Review & Editing.

# **REFERNCES**

- Vinoth Kumar J, Karthik R, Shen-Ming Chen, Balasubramanian P, Muthuraj P, Selvam V. A Novel Cerium Tungstate Tanosheets Modified Electrode for the Effective Electrochemical Detection of Carcinogenic Nitrite Ions. Electroanalysis. 2017; 29: 2385-2394.
- Chengyi Hong, Dandan Li, Siying Cao, Xin Huang, Hongfen Yang, Dan Yang, et al. Sensitive and Multicolor Detection of Nitrite Based on Iodide-Mediated Etching of Gold Nanostars. Chem Commun. 2022; 58: 12983-12986.
- 3. Wang XF, Fan JC, Ren R, Jin Q, Wang J. Rapid determination of nitrite in foods in acidic conditions by high performance liquid



- chromatography with fluorescence detection. J Sep Sci. 2016; 39: 2263-2269
- Lingzhi He, Wu Zo, Dan Zeng, Fuchun Gong, Qinge Wang, Jiaoyun Xia, et al. Highly Fluorescent Dihydropyrimido-Diindole Derivative as a Probe for Detecting Nitrite in Food Products and Cell-Imaging. Dyes Pigments. 2020; 177: 1082-1056.
- Wang QH, Yu LJ, Liu Y, Lin L, Lu RG, Zhu JP, et al. Methods for the detection and determination of nitrite and nitrate: A review. Talanta. 2017; 165: 709-720.
- Hu Y, Shen L, Zhang Y, Lu L, Fu H, She Y. A naphthalimide-based fluorescent probe for rapid detection of nitrite and its application in food quality monitoring. Anal Chim Acta. 2023; 1268: 341403.
- Minghui Zan, Cong Li, Fei Liao, Lang Rao, Qian-Fang Meng, Wei Xie, et al. One-Step Synthesis of Green Emission Carbon Dots for Selective and Sensitive Detection of Nitrite Ions and Cellular Imaging Application. RSC Adv. 2020; 10: 10067-10075.
- 8. Chen Y, Zhao C, Yue G, Yang Z, Wang Y, Rao H, et al. A highly selective chromogenic probe for the detection of nitrite in food samples. Food Chem. 2020; 317: 126361.
- Meiyi Cai, Xiaoyun Chai, Xuedong Wang, Ting Wang. An Acid-Inert Fluorescent Probe for the Detection of Nitrite. J. Fluoresc. 2017; 27: 1365-1371.
- Yang L, Wang F, Zhao J, Kong X, Lu K, Yang M, et al. A facile dualfunction fluorescent probe for detection of phosgene and nitrite and its applications in portable chemosensor analysis and food analysis. Talanta. 2021; 221: 121477.
- Lloyd C. Murfin, Carlos M. López-Alled, Adam C. Sedgwick, Jannis Wenk, Tony D. James, Simon E. Lewis. A Simple, Azulene-Based Colorimetric Probe for the Detection of Nitrite in Water. Front Chem Sci Eng.2019; 14: 90-96.
- Jianqiang Song, Sitong Liu, Ning Zhao, Longshan Zhao. A New Fluorescent Probe Based on Metallic Deep Eutectic Solvent for Visual Detection of Nitrite and Ph in Food and Water Environment. Food Chem. 2023; 398: 133935.
- 13. Na Wei, Meng-Xia Wei, Bo-Hui Huang, Xiao-Feng Guo, Hong Wang. One-Pot Facile Synthesis of Green-Emitting Fluorescent Silicon Quantum Dots for the Highly Selective and Sensitive Detection of Nitrite in Food Samples. Dyes Pigments. 2021; 184: 108848.
- 14. Muthaiah Annalakshmi, Sakthivel Kumaravel, Shen-Ming Chen, Paramasivam Balasubramanian, T.S.T. Balamurugan. A Straightforward Ultrasonic-Assisted Synthesis of Zinc Sulfide for Supersensitive Detection of Carcinogenic Nitrite Ions in Water Samples. Sensor Actuat. B-chem. 2020; 305: 127387.
- 15. Yilmaz MD. A novel ratiometric and colorimetric probe for rapid and ultrasensitive detection of nitrite in water based on an Acenaphtho[1,2-d] imidazole derivative. Anal Chim Acta. 2021; 1166: 338597.
- Jing Fang Tan, Amie Anastasi, Shaneel Chandra. Electrochemical Detection of Nitrate, Nitrite and Ammonium for On-Site Water Quality Monitoring. Curr Opin Electroche. 2022; 32: 100926.
- 17. Wang X, Adams E, Van Schepdael A. A fast and sensitive method for the determination of nitrite in human plasma by capillary electrophoresis with fluorescence detection. Talanta. 2012; 97: 142-144.
- 18. Lo HS, Lo KW, Yeung CF, Wong CY. Rapid visual and spectrophotometric nitrite detection by cyclometalated ruthenium complex. Anal Chim Acta. 2017; 990: 135-140.
- 19. Singh L, Ranjan N. Highly Selective and Sensitive Detection of Nitrite

- Ion by an Unusual Nitration of a Fluorescent Benzimidazole. J Am Chem Soc. 2023; 145: 2745-2749.
- 20. Haimin Zhang, Shenghong Kang, Guozhong Wang, Yunxia Zhang, Huijun Zhao. Fluorescence Determination of Nitrite in Water Using Prawn-Shell Derived Nitrogen-Doped Carbon Nanodots as Fluorophores. ACS Sensors. 2016; 1: 875-881.
- Carneiro SV, Oliveira JJP, Rodrigues VSF, Fechine LMUD, Antunes RA, Neto MLA, et al. Doped Carbon Quantum Dots/PVA Nanocomposite as a Platform to Sense Nitrite Ions in Meat. ACS Appl Mater Interfaces. 2022: 14: 43597-43611.
- 22. Jing Xu, Yanfeng Shi, Shanshan Yang, Jinliang Yang, Xue Zhang, Lirong Xu, et al. Highly Selective Colorimetric Fluorescent Probe for Detecting Nitrite in Aqueous Solution. Microchem J. 2021; 169: 106342.
- Huihui Wang, Nanwei Wan, Lin Ma, Zhongqiang Wang, Baodong Cui, Wenyong Han, et al. A Novel and Simple Spectrophotometric Method for Detection of Nitrite in Water. Analyst. 2018; 143: 4555-4558.
- Kang SH, Chung BY, Park JE, Jeon J, Park YD. Activatable red emitting fluorescent probe for rapid and sensitive detection of intracellular peroxynitrite. Talanta. 2020; 217: 121053.
- Zhang F, Zhu X, Jiao Z, Liu X, Zhang H. Sensitive naked eye detection and quantification assay for nitrite by a fluorescence probe in various water resources. Spectrochim Acta A Mol Biomol Spectrosc. 2018; 200: 275-280.
- 26. Ke Wu, Wenjie Yang, Zhi Yan, Haichao Wang, Zhijuan Zheng, Anqi Jiang, et al. Accurate Quantification, Naked Eyes Detection and Bioimaging of Nitrite Using a Colorimetric and Near-Infrared Fluorescent Probe In Food Samples and Escherichia Coli. Spectrochim. Acta A Mol Biomol Spectrosc. 2022; 282: 121692.
- 27. Matheus Fernandes Filgueiras, Paulo Cesar de Jesus, Endler Marcel Borges. Quantification Of Nitrite in Food and Water Samples Using the Griess Assay and Digital Images Acquired Using a Desktop Scanner. J Chem Edu. 2021; 98: 3303-331.
- 28. Shen Y, Zhang Q, Qian X, Yang Y. Practical assay for nitrite and nitrosothiol as an alternative to the Griess assay or the 2,3-diaminonaphthalene assay. Anal Chem. 2015; 87: 1274-1280.
- Jianhua Wang, Jingying Yang, Chuan Dong, Yu Wang, Shaomin Shuang. A Smartphone-Adaptable Dual-Signal Readout Chemosensor for Rapid Detection of Nitrite in Food Samples. J Food Compos Anal. 2023; 118: 105179.
- 30. Qiuhua Wang, Sufang Ma, Haiwei Huang, Aocheng Cao, Minfeng Li, Lan He. Highly Sensitive and Selective Spectrofluorimetric Determination of Nitrite in Food Products with a Novel Fluorogenic Probe. Food Control. 2016; 63: 117-121.
- 31. Jian Zhang, Fuchao Pan, Yue Jin, Nannan Wang, Jinling He, Weijuan Zhang, et al. A BODIPY-Based Dual-Responsive Turn-On Fluorescent Probe for NO and Nitrite. Dyes Pigments. 2018; 155: 276-283.
- 32. Virgyl Camberlein, Nicolas Kraupner, Nour Bou Karroum, Emmanuelle Lipka, Rebecca Deprez-Poulain, Benoit Deprez, et al. Multi-Component Reaction for the Preparation Of 1,5-Disubstituted 1,2,3-Triazoles by In-Situ Generation of Azides and Nickel-Catalyzed Azide-Alkyne Cycloaddition. Tetrahedron Lett. 2021; 73: 153131.
- Strianese M, Milione S, Bertolasi V, Pellecchia C. Iron and manganese pyridoxal-based complexes as fluorescent probes for nitrite and nitrate anions in aqueous solution. Inorg Chem. 2013; 52: 11778-11786
- 34. Ma Z, Li J, Hu X, Cai Z, Dou X. Ultrasensitive, Specific, and Rapid Fluorescence Turn-On Nitrite Sensor Enabled by Precisely Modulated Fluorophore Binding. Adv Sci (Weinh). 2020; 7: 2002991.

# **SciMed**Central

- 35. Xu Z, Shi W, Yang C, Xu J, Liu H, Xu J, et al. A colorimetric fluorescent probe for rapid and specific detection of nitrite. Luminescence. 2020; 35: 299-304.
- Gu B, Huang L, Hu J, Liu J, Su W, Duan X, et al. Highly selective and sensitive fluorescent probe for the detection of nitrite. Talanta. 2016; 152: 155-161.
- Qiuhua Wang, Haiwei Huang, Baoming Ning, Minfeng Li, Lan He. A Highly Sensitive and Selective Spectrofluorimetric Method for the Determination of Nitrite in Food Products. Food Anal Methods. 2015: 9: 1293-1300.
- 38. Cao GP, Yang RY, Zhuang YF, Zuo D, Wang YH. Simple and sensitive determination of trace nitrite in water by zero-crossing first-derivative synchronous fluorescence spectrometry using 6-amino-1,3- naphthalenedisulfonic acid as a new fluorescent probe. Anal Bioanal Chem. 2017; 409: 4637-4646.
- Feng R, Fan Y, Fang Y, Xia Y. Morphological Effects of Au Nanoparticles on Electrochemical Sensing Platforms for Nitrite Detection. Molecules. 2023; 28: 4934.
- Jia J, Lu WJ, Li L, Jiao Y, Gao YF, Shuang SM. Orange Luminescent Carbon Dots as Fluorescent Probe for Detection of Nitrite. Chin. J Anal.Chem. 2019; 47: 560-566.
- 41. Kong Y, Cheng Q, He Y, Ge Y, Zhou J, Song G. A dual-modal fluorometric and colorimetric nanoprobe based on graphitic carbon nitrite quantum dots and Fe (II)-bathophenanthroline complex for detection of nitrite in sausage and water. Food Chem. 2020; 312: 126089
- Xiaohui Hao, Yueqi Liang, Hao Zhen, Xinchao Sun, Xueliang Liu, Mengwen Li, et al. Fast and Sensitive Fluorescent Detection of Nitrite Based on an Amino-Functionalized Mofs of Uio-66-NH<sub>2</sub>. J Solid State Chem. 2020; 287: 287-291.
- 43. Zhu Su, Xinyi Wang, Minchuan Luo, Liang Li, Yifeng Tu, Jilin Yan. Fluorometric Determination of Nitrite Through Its Catalytic Effect on

- the Oxidation of Iodide and Subsequent Etching of Gold Nanoclusters By Free Iodine. Mikrochim Acta. 2019: 186: 619.
- 44. Ren HH, Fan Y, Wang B, Yu LP. Polyethylenimine-Capped CdS Quantum Dots for Sensitive and Selective Detection of Nitrite in Vegetables and Water. J Agric Food Chem. 2018; 66: 8851-8858.
- 45. Weijie Wang, Shifen Xu, Ning Li, Zhiyong Huang, Bingyuan Su, Xiaomei Chen. Sulfur and Phosphorus Co-Doped Graphene Quantum Dots for Fluorescent Monitoring of Nitrite in Pickles. Spectrochim. Acta A Mol Biomo Spectrosc. 2019; 221: 117211.
- Tsuyoshi Taniguchi, Atsushi Yajima, Hiroyuki Ishibashi. Oxidative Nitration of Alkenes with Tert-Butyl Nitrite and Oxygen. Adv Synth Catalysis. 2011; 14: 2643-2647.
- Hao X, Shen A, Li M, Duan R, Hou L, Zhao X, et al. Simple method for visual detection of nitrite using fluorescence and colorimetry by poly (tannic acid) nanoparticles. Anal Chim Acta. 2023; 1263: 341280.
- 48. Giustarini D, Dalle-Donne I, Colombo R, Milzani A, Rossi R. Adaptation of the Griess reaction for detection of nitrite in human plasma. Free Radic Res. 2004; 38: 1235-1240.
- Wu H, Shen X, Huo D, Ma Y, Bian M, Shen C, et al. Fluorescent and colorimetric dual-readout sensor based on Griess assay for nitrite detection. Spectrochim Acta A Mol Biomol Spectrosc. 2020; 225: 117470.
- Aydın A, Ercan O, Taşcıoğlu S. A novel method for the spectrophotometric determination of nitrite in water. Talanta. 2005; 66: 1181-1186.
- Li Q, Liu R, Shang Y, Wei Y, Cui H. Study on Nitrite Nitrogen Based on Ultraviolet Visible Absorption Spectrometry. Academic J Sci Technol. 2023: 5: 2771-3032.
- 52. GB 2762-2017, Maximum Levels of Contaminants in Foods, National Food Safety Standard of the People's Republic of China, Standards Press of China, Beijing 2017.